nature metabolism

Article

https://doi.org/10.1038/s42255-023-00816-9

Brain responses to nutrients are severely impaired and not reversed by weight loss in humans with obesity: a randomized crossover study

Received: 12 February 2023

Accepted: 4 May 2023

Published online: 12 June 2023

Check for updates

Katy A. van Galen[1], Anouk Schrantee[1], Kasper W. ter Horst[2], Susanne E. la Fleur[2,3], Jan Booij[1], R. Todd Constable[4], Gary J. Schwartz[5], Ralph J. DiLeone[6] & Mireille J. Serlie[2,7]

Post-ingestive nutrient signals to the brain regulate eating behaviour in rodents, and impaired responses to these signals have been associated with pathological feeding behaviour and obesity. To study this in humans, we performed a single-blinded, randomized, controlled, crossover study in 30 humans with a healthy body weight (females $N = 12$, males $N = 18$) and 30 humans with obesity (females $N = 18$, males $N = 12$). We assessed the effect of intragastric glucose, lipid and water (noncaloric isovolumetric control) infusions on the primary endpoints cerebral neuronal activity and striatal dopamine release, as well as on the secondary endpoints plasma hormones and glucose, hunger scores and caloric intake. To study whether impaired responses in participants with obesity would be partially reversible with diet-induced weight loss, imaging was repeated after 10% diet-induced weight loss. We show that intragastric glucose and lipid infusions induce orosensory-independent and preference-independent, nutrient-specific cerebral neuronal activity and striatal dopamine release in lean participants. In contrast, participants with obesity have severely impaired brain responses to post-ingestive nutrients. Importantly, the impaired neuronal responses are not restored after diet-induced weight loss. Impaired neuronal responses to nutritional signals may contribute to overeating and obesity, and ongoing resistance to post-ingestive nutrient signals after significant weight loss may in part explain the high rate of weight regain after successful weight loss.

The orosensory effects of food have long been identified as the primary driving force behind food intake beyond homeostatic needs[1,2]. In addition to the palatability of nutrients, increasing evidence shows a potent role for signals that arise after the ingestion of food—so-called post-ingestive nutrient signals—in the regulation of eating behaviour[3]. For instance, *Trpm5*$^{-/-}$ mice that lack sweet taste transduction still develop a clear preference for sucrose over noncaloric solutions[4], indicating a calorie-dependent and taste-independent effect on food intake. Other studies show that mice are receptive to appetition, the process of flavour conditioning associated with intragastric infusion of nutrients[5,6].

A full list of affiliations appears at the end of the paper. e-mail: mireille.serlie@yale.edu

https://doi.org/10.1038/s42255-023-00816-9

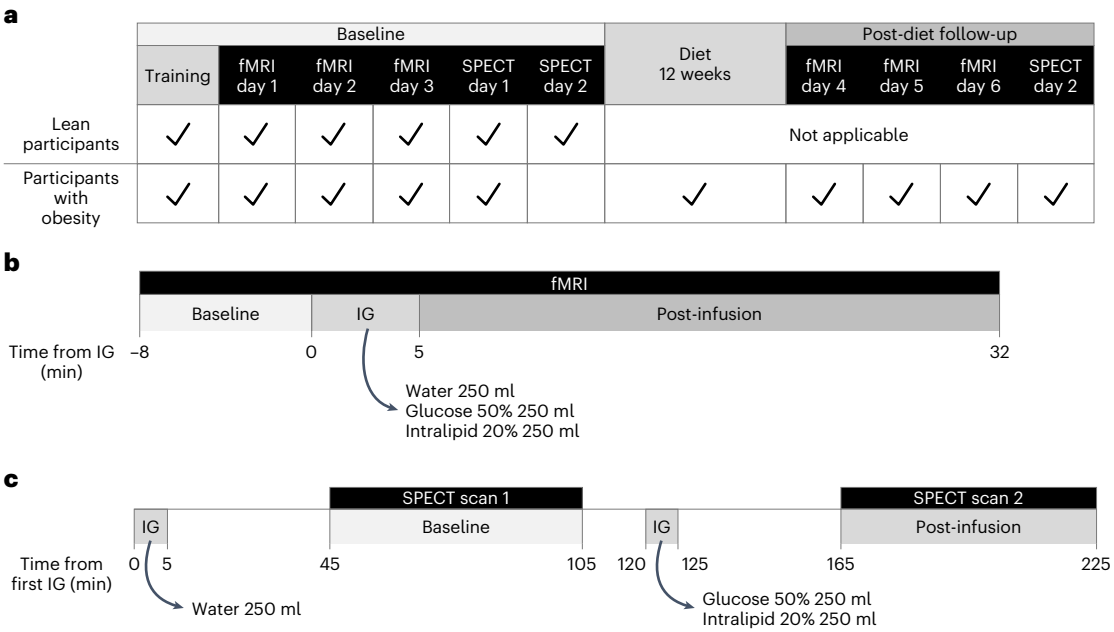

Fig. 1 | Schematics of the study design and main study procedures. a, Overview of the study design and overall timing of procedures in the lean participants and participants with obesity. Each imaging session was performed on a separate study day, and the order of sessions (that is, to assess the effects of intragastric (IG) glucose, lipids or water) was randomized. **b**, Overview of an fMRI study day. **c**, Overview of a SPECT imaging study day.

Several post-ingestive nutrient signals convey the presence of nutrients in the gastrointestinal tract to the brain and may contribute to the regulation of eating behaviour via the gut–brain axis. Firstly, gastrointestinal vagal nerve afferents are stimulated upon the presence of nutrients and mediate anorexigenic effects via the brainstem to several downstream brain regions[7,8]. Secondly, nutrients in the gastrointestinal lumen induce an endocrine response and facilitate the digestion, absorption and subsequent metabolism of nutrients. The post-ingestive endocrine response includes, but is not limited to, enhanced release of insulin from pancreatic beta cells, glucagon-like peptide-1 (GLP-1) from intestinal L cells[9,10], and suppressed release of ghrelin from gastric X/A-like cells[11]. Gastrointestinal vagal nerve afferents and multiple brain regions express receptors for these hormones, but the exact mechanisms by which insulin and GLP-1 mediate anorexigenic effects and ghrelin mediates orexigenic effects remain to be elucidated[12]. Finally, changes in the concentrations of nutrients and/or metabolites in the portal or systemic circulation provide a direct post-ingestive signal of nutrient availability for different brain regions involved in the central regulation of food intake[13,14].

While the post-ingestive signals induced by glucose versus lipid consumption differ in several aspects, administration of both carbohydrate and lipid promotes the release of striatal dopamine in rodents[7,15]. The striatum is involved in the rewarding and motivational aspects of food intake[7,13]. A study in humans without obesity reported a biphasic striatal dopamine response immediately and approximately 20 min following the consumption of a milkshake solution, which was hypothesized to reflect both an immediate orosensory and delayed post-ingestive response[16]. In rodents, striatal dopamine release is positively and proportionally related to intragastric fat infusions, and intact striatal dopamine signalling is required to reduce subsequent caloric intake in proportion to the amount of fat directly infused into the stomach[17]. Interestingly, long-term exposure to a high-fat diet resulted in an impaired striatal dopaminergic response to an intragastric lipid infusion[18]. Taken together, these studies demonstrate that, (i) in addition to direct gustatory effects of nutrients, post-ingestive nutrient signals contribute to the regulation of feeding behaviour; and (ii) impaired striatal dopamine signalling after prolonged exposure to high-calorie nutrients may promote subsequent overeating and obesity.

Despite these intriguing mostly preclinical studies, little is known about the role of post-ingestive nutrient signals in human physiology or obesity development. A few studies have assessed the response of the brain to the isolated, orosensory-independent, post-ingestive effects of glucose or dodecanoate (a C12 fatty acid) by means of intragastric infusions using functional magnetic resonance imaging (fMRI)[19–21]. The intragastric glucose infusion decreased blood oxygen level-dependent (BOLD) signal in the striatum and several other brain regions, including the brainstem, hypothalamus and thalamus[19]. The intragastric dodecanoate infusion increased BOLD signal in the brainstem, pons, hypothalamus, cerebellum and motor cortical areas[20,21]. However, these studies were conducted in participants without obesity and did not assess the effect of such intragastric infusions on striatal dopamine release.

Given the devastating impact of obesity worldwide, it is highly relevant to determine whether post-ingestive nutrient signals and/or the subsequent striatal dopamine response are impaired in humans with obesity. On the basis of the available data, we hypothesized that intragastric infusions of glucose and lipid modulate cerebral neuronal activity and striatal dopamine release in lean humans and that these responses are impaired in humans with obesity. Finally, we hypothesized that an impaired response to post-ingestive nutrient signals is partially reversible with diet-induced weight loss. In this regard, we have previously demonstrated that obesity-associated changes in the striatal dopamine system are partially reversed by bariatric surgery-induced weight loss in women[22].

To test our hypotheses, we recruited lean individuals and individuals with obesity and evaluated the effects of direct, intragastric infusions of tap water (isovolumetric and noncaloric control), glucose and lipids on cerebral neuronal activity using fMRI and on striatal dopamine release using single-photon emission computed tomography (SPECT) imaging (Fig. 1). Participants with obesity were studied before and after a dietary intervention aimed at reducing body weight by 10%.

https://doi.org/10.1038/s42255-023-00816-9

Table 1 | Baseline characteristics of study participants (n=58)

		Participants with obesity				
	Lean participants (n=28)	Pre-diet (n=30)	P^a	Post-diet (n=26)	Change from pre-diet (%)	P^b
Sex (male:female)	17:11	12:18	0.115			
Age (years)	60±9	58±7	0.283			
Weight (kg)	71.0±10.9	100.8±17.7	<0.001	90.3±15.5	−9.5±2.8	<0.001
BMI (kg/m^2)	23.0 (22.0–24.4)	32.6 (31.1–36.9)	<0.001	29.4 (28.4–32.9)	−9.5±2.7	<0.001
Body fat (%)	21.7±8.3	42.9±8.2	<0.001	37.8±8.8	−13.4±7.6	<0.001
Waist circumference (cm)	87±11	116±12	<0.001	105±10	−9.3±3.8	<0.001
REE (kcal/day)	1,501±240	1,706±333	0.010	1,676±318	1.1±12.7	0.802
RQ	0.79±0.05	0.80±0.04	0.377	0.82±0.11	2.2±11.8	0.400
Fasting glucose (mmol l^{-1})	4.9±0.3	5.3±0.6	0.001	4.9±0.3	−6.6±6.0	<0.001
Fasting insulin (pmol l^{-1})	33±24	65±44	0.001	45±25	−19.0±33.3	0.001
Fasting acylated ghrelin (pg ml^{-1})	56 (38–91)	36 (17–64)	0.028	56 (36–75)	44.9±67.1	0.090
Fasting total GLP-1 (pmol l^{-1})	8.8±2.5	8.5±3.0	0.711	6.4±1.6	−16.1±20.8	<0.001

Data are the count, mean±s.d. or median (interquartile range). REE, resting energy expenditure; RQ, respiratory quotient.
[a]Lean participants versus pre-diet participants with obesity by two-sided t-test, Mann–Whitney U test or chi-square test as appropriate (n=55–58).
[b]Change from pre-diet by two-sided paired t-tests or Wilcoxon signed-rank test (n=25–26).

Results

Obesity-related insulin resistance improved with weight loss

Twenty-eight lean participants with body mass index (BMI) ≤ 25 kg/m^2 and 30 participants with obesity and BMI ≥ 30 kg/m^2 were included in the analysis (Table 1 and Fig. 2). In line with our expectations, obesity was associated with increased fasting glucose and insulin concentrations, indicating insulin resistance[23], and with decreased fasting ghrelin at baseline[24,25]. Following the baseline assessments, participants with obesity enrolled in a supervised personalized dietary weight loss programme aimed at reducing body weight by 10% over a period of 12 weeks. Twenty-six participants with obesity completed the dietary intervention. As shown in Table 1, the intervention was successful at promoting the intended weight and body fat loss. Notably, dietary weight loss was not associated with a decrease in resting energy expenditure (REE), suggesting maintenance of lean body mass[26], and it was associated with improved insulin sensitivity, as reflected by decreased fasting glucose and insulin[27]. In addition, dietary weight loss was associated with a decrease in fasting GLP-1 to levels below those observed in the lean participants.

Post-ingestive metabolic response to intragastric nutrients

To evaluate the metabolic and cerebral effects of post-ingestive nutrient signals, we used direct intragastric infusions of glucose (125 g in 250 ml of water; 500 kcal), lipid (250 ml of 20% Intralipid; 500 kcal) or water (250 ml of tap water; noncaloric isovolumetric control). Participants underwent all studies in a random assignment and crossover design. They were blinded for the type of infusion, and the infusions were administered via nasogastric tube to eliminate all anticipatory and orosensory effects. This design allowed us to specifically isolate the post-ingestive effects of these nutrients.

As expected, intragastric glucose infusions rapidly and strongly raised plasma glucose and insulin concentrations in all participants, whereas intragastric lipid infusions only slightly increased circulating insulin (Fig. 3a,b). Glucose and lipid infusions decreased acylated ghrelin and increased total GLP-1 levels in both groups (Fig. 3c,d). Overall, these data show an evident metabolic response within the first 30 min after the intragastric infusion, which is when we assessed cerebral responses using fMRI.

In addition, we evaluated the effects of the intragastric infusions on feelings of hunger (visual analogue scale (VAS) scores) and subsequent ad libitum caloric intake. Independent of the nature of the intragastric infusion, lean participants and participants with obesity in the pre-diet condition did not report decreased hunger scores after the fMRI scan (VAS −0.1 ± 1.8, P = 0.303); in the participants with obesity, this did not change following the dietary intervention (VAS 0.1 ± 1.8, P = 0.649). However, this secondary outcome measure may have been underpowered[28]. The number of calories consumed by lean participants did not depend on the nature of the received intragastric infusion (P = 0.401). Compared to lean participants, participants with obesity consumed more calories in the pre-diet condition (pre-diet 538 kcal versus lean 404 kcal, P = 0.013) and this did not change following the diet (pre-diet 529 kcal versus post-diet 543 kcal, P = 0.531).

Post-ingestive brain activity is blunted in individuals with obesity

To evaluate the isolated post-ingestive effects of glucose and lipid on brain activity, participants underwent three separate fMRI scanning sessions following the intragastric infusion of glucose, lipid and water (control; Fig. 1b). During each fMRI scan, the whole-brain BOLD response was continuously measured for a duration of 40 min. The BOLD signal is the local ratio of deoxyhaemoglobin to oxyhaemoglobin, based on increased cerebral blood flow in response to neuronal activity[29]. Eight minutes after the start of the fMRI scan, participants received the intragastric glucose, lipid or water infusion (250 ml in 5 min). We used exploratory voxel-wise and targeted region-of-interest (ROI) analyses to compare whole-brain and striatal BOLD signal responses to the intragastric infusions, respectively.

We first performed a whole-brain voxel-wise analysis to identify the typical cerebral BOLD signal response to intragastric glucose or lipids (both corrected for the BOLD response to intragastric water) in humans with normal body weight. Our data show that glucose and lipid both induce multiple post-ingestive effects on brain activity in lean participants (Table 2). We observed decreased BOLD signal in striatal, frontal, insular, limbic, occipital, parietal and temporal regions at 10 to 15 min after the intragastric glucose infusion (that is, time bins T5 and T6); a more prolonged neuronal response was observed in the nucleus accumbens (NAc), putamen and frontal pole (Table 2 and

https://doi.org/10.1038/s42255-023-00816-9

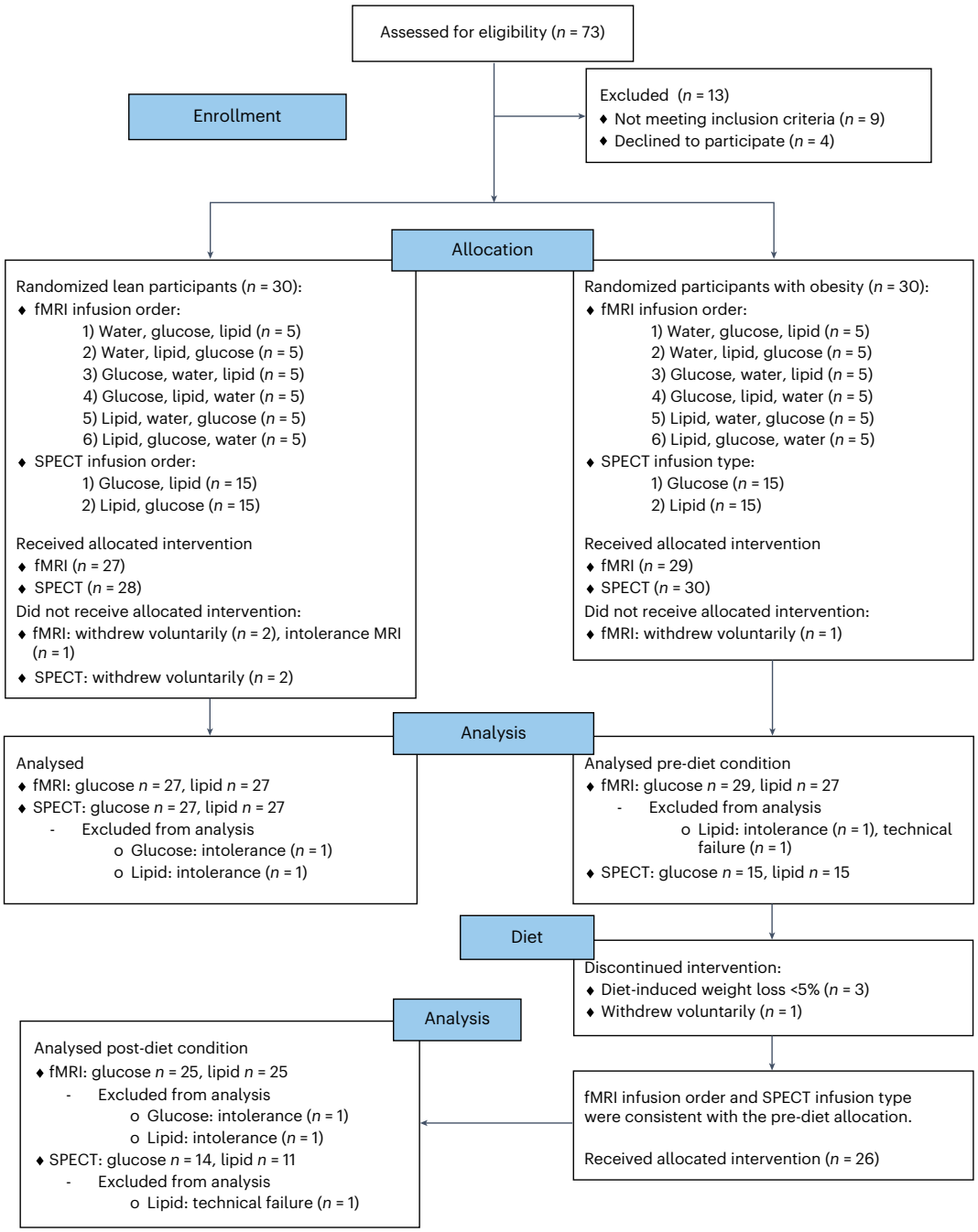

Fig. 2 | Participant flow diagram. Overview of the number of screened and randomized participants.

Supplementary Table 1). In contrast, after the intragastric lipid infusion, we observed decreases in BOLD signal in frontal, insular, limbic, parietal and temporal regions at 20 to 22.5 min (that is, time bin T9); here, a more prolonged response was observed in frontal, insular and parietal regions and a delayed response was observed in the occipital lobe (Table 2 and Supplementary Table 2). Importantly, whole-brain voxel-wise analyses revealed no significant nutrient-induced changes in BOLD signal in any region in the participants with obesity, and there were no differences between the pre-diet and post-diet conditions (Table 2 and Supplementary Tables 1 and 2). These data indicate that brain regions involved in the regulation of eating behaviour respond in a nutrient-specific manner to the post-ingestive effects of glucose and lipid. Moreover, our observations that this physiological response is absent in participants with obesity and is not restored following diet-induced weight loss suggest that impaired post-ingestive nutrient sensing may play a role in obesity and may also contribute to the high rate of weight regain after diet-induced weight loss.

Impaired post-ingestive striatal responses are not reversible with weight loss

The striatum has an essential role in the regulation of eating behaviour[17]. It has been proposed to also function as a post-ingestive caloric sensor, and it coordinates an appropriate behavioural response to nutrient exposure[17]. Therefore, we complemented the explorative voxel-wise analysis with a targeted ROI analysis to test our hypothesis that obesity is associated with a blunted striatal response to post-ingestive nutrient

https://doi.org/10.1038/s42255-023-00816-9

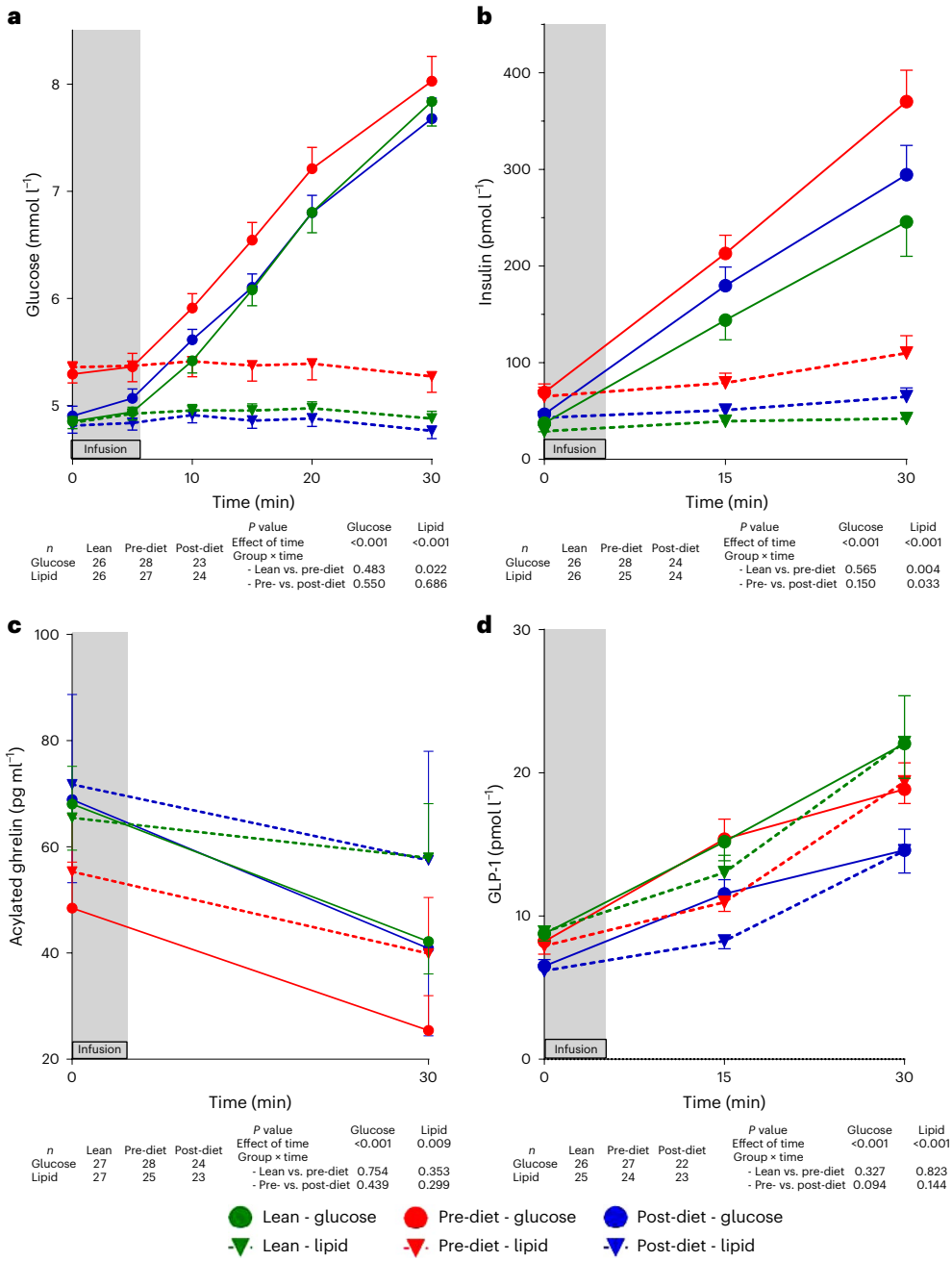

Fig. 3 | Effect of intragastric glucose and lipid infusions on glucose, insulin and gut hormones. a, Plasma glucose. **b**, Plasma insulin. **c**, Plasma acylated ghrelin. **d**, Total plasma GLP-1. Green symbols indicate lean participants; red and blue symbols indicate participants with obesity before and after weight loss, respectively. Data are the mean ± s.e.m. and compared by analysis of variance (ANOVA). Effect of time was assessed in lean participants and participants in the pre-diet condition. The interaction between time and group was assessed for lean versus pre-diet and pre-diet versus post-diet.

signals. To this end, we assessed the post-ingestive effects of glucose and lipids on the BOLD signal in striatal subregions in lean participants and participants with obesity before versus after weight loss.

The intragastric administration of both glucose and lipid to lean participants induced strong decreases in BOLD signal in both the NAc and the putamen (Fig. 4a,b and Supplementary Table 3). We observed no post-ingestive effects on the caudate nucleus (Fig. 4c and Supplementary Table 3). This physiological cerebral response to these nutrients was severely impaired in participants with obesity: there were no changes in BOLD signal in any of the striatal subregions, except for an intragastric glucose-induced effect in the putamen (Fig. 4a–c and Supplementary Table 3). More importantly, dietary weight loss in the participants with obesity was not associated with a restoration of the cerebral responses to post-ingestive nutrient signals (Fig. 4a–c and Supplementary Table 3). A direct (paired) comparison between the BOLD signal responses in the participants before versus after the dietary intervention revealed no significant differences in any striatal region. Taken together, these data show that the striatal response to post-ingestive nutrient signals is impaired and not reversible with significant weight loss in humans with obesity.

Striatal dopamine release is impaired in humans with obesity

The neurotransmitter dopamine is involved in the motivational and rewarding aspects of food intake. In the context of obesity, blunted

https://doi.org/10.1038/s42255-023-00816-9

Table 2 | The 'lean brain phenotype'

Time bin		T1	T2	T3	T4	T5	T6	T7	T8	T9	T10	T11	T12	T13
Time since intragastric infusion (min)		0		5		10		15		20		25		30
Striatum	Nucleus accumbens							●		●				
	Putamen					●	●	●	●	●				
Frontal lobe	Inferior frontal gyrus, pars opercularis						●			▼		▼	▼	▼
	Inferior frontal gyrus, pars triangularis					●	●							
	Middle frontal gyrus					●								
	Frontal orbital cortex						●			▼			▼	▼
	Frontal medial cortex					●								
	Frontal pole					●	●		●	●▼				▼
	Frontal operculum									▼				
	Precentral gyrus									▼				
Insula	Insular cortex						●			▼			▼	▼
Limbic lobe	Cingulate gyrus, anterior division						●							
	Hippocampus									▼				
	Paracingulate gyrus					●								
	Subcallosal cortex					●	●							
Occipital lobe	Cuneal cortex					●								
	Lateral occipital cortex, inferior division					●	●							
	Lateral occipital cortex, superior division					●							▼	▼
	Occipital fusiform gyrus					●								
	Occipital pole					●								▼
Parietal lobe	Angular gyrus					●▼								▼
	Postcentral gyrus									▼				
	Precuneous cortex									▼				▼
	Superior parietal lobule					●				▼				▼
	Supramarginal gyrus, anterior division					●	●							
	Supramarginal gyrus, posterior division						●							
Temporal lobe	Inferior temporal gyrus, temporooccipital division					●								
	Inferior temporal gyrus, posterior division													▼
	Middle temporal gyrus, posterior division					●	●			▼				
	Middle temporal gyrus, temporooccipital division					●								
	Superior temporal gyrus, posterior division					●	●							

Multiple brain regions show a significant decrease in BOLD signal at various intervals after the intragastric infusion of glucose (●), lipids (▼) or both (●▼) in lean participants (n=27). In participants with obesity, no brain regions showed a change in BOLD signal after an intragastric nutrient infusion; this did not change following weight loss. Neuronal activity within each time bin (T) was compared to neuronal activity at T0 (that is, baseline after an overnight fast). Clusters were identified using Threshold Free Cluster Enhancement and permutation testing, with P values corrected for the family-wise error rate (FWER) for the multiple contrasts and time bins. We used the Harvard–Oxford (sub)cortical atlas for the localization of BOLD signal clusters.

dopaminergic responses to nutrients have been suggested to contribute to energy consumption beyond homeostatic needs. Thus, to test our hypothesis—that post-ingestive glucose and lipid induce striatal dopamine release in lean participants, but not in participants with obesity—we measured striatal dopamine release in response to intragastric glucose and lipids (Fig. 1c). To this end, we applied SPECT imaging in combination with the radiotracer [^{123}I]-iodobenzamide ([^{123}I]IBZM) to determine striatal dopamine $D_{2/3}$ receptor ($D_{2/3}$R) availability at baseline and after nutrient infusions (Fig. 5a). Given that acute changes in $D_{2/3}$R availability in response to a stimulus are a measure of striatal dopamine release[30], this design allowed us to determine the post-ingestive effects of glucose and lipids on striatal dopamine release in humans in vivo.

Intragastric infusion of glucose induced striatal dopamine release in all groups, with no group differences between the lean participants and those with obesity (Fig. 5b). In contrast, intragastric infusion of lipid induced striatal dopamine release in lean participants only. In the participants with obesity, this impaired dopaminergic response to lipid was not reversible with diet-induced weight loss (Fig. 5c). These data

https://doi.org/10.1038/s42255-023-00816-9

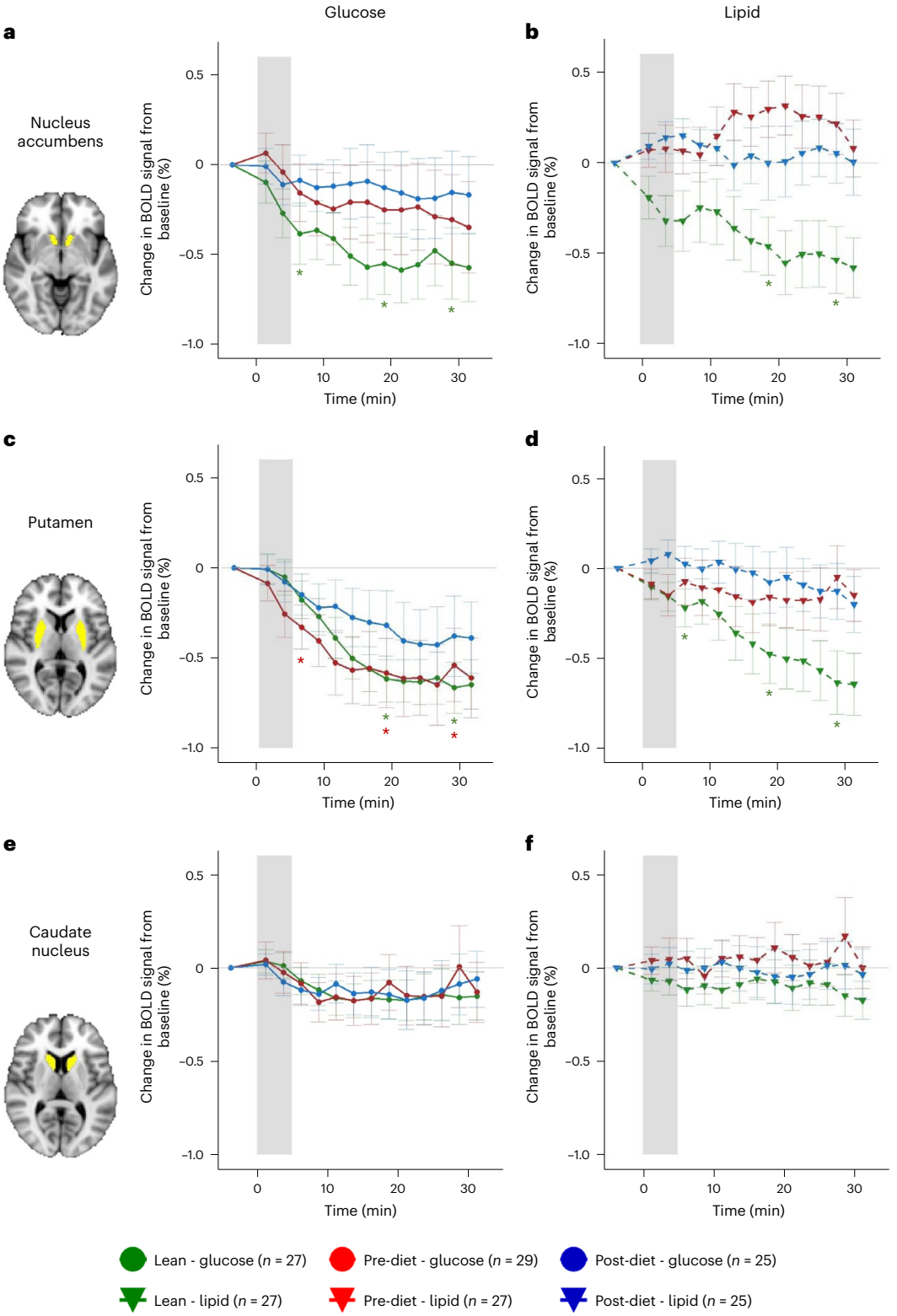

Fig. 4 | BOLD signal following intragastric glucose and lipid infusions (controlled for intragastric water infusions) in lean participants and participants with obesity before and after weight loss. a,**b**, Changes in NAc BOLD signal over time after intragastric glucose (**a**) or lipid (**b**) administration. **c**,**d**, Changes in putamen BOLD signal over time after intragastric glucose (**c**) or lipid (**d**) administration. **e**,**f**, Changes in caudate nucleus BOLD signal over time after intragastric glucose (**e**) or lipid (**f**) administration. Data are the mean ± s.e.m. Green symbols indicate lean participants; red and blue symbols indicate participants with obesity before and after weight loss, respectively. Grey shaded area indicates the time frame (5 min) of intragastric infusion. Credits for images at left: ROI masks were obtained from the Harvard–Oxford subcortical atlas[64–67] and are shown overlaid on a MNI152 brain (Copyright (C) 1993–2009 Louis Collins, McConnell Brain Imaging Centre, Montreal Neurological Institute, McGill University)[73]. *$P < 0.05$ versus baseline (two-sided one-sample t-test). The exact P values are available in Supplementary Table 3.

https://doi.org/10.1038/s42255-023-00816-9

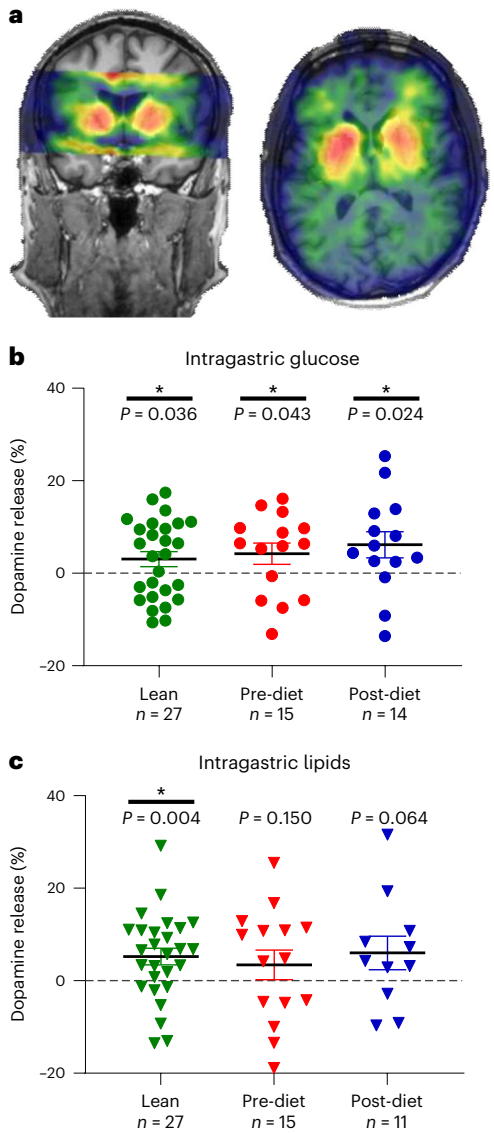

Fig. 5 | Dopamine release following intragastric glucose and lipid infusions in lean participants and participants with obesity before and after weight loss. **a**, Representative example of a T1-weighted anatomical brain MRI overlaid with the co-registered SPECT image of a lean participant showing the distribution of radiotracer uptake, with strongest uptake of [^{123}I]IBZM in the bilateral striata. **b**, Post-ingestive effects of glucose on striatal dopamine release. **c**, Post-ingestive effects of lipids on striatal dopamine release. Nutrient-induced striatal dopamine release (percentage) was calculated as: the percentage change in striatal [^{123}I]IBZM $BP_{ND} \times -1$. Data are individual participants with mean ± s.e.m. $^*P < 0.05$ versus baseline (one-sided one-sample *t*-tests).

suggest that striatal dopamine release is not nutrient specific in lean participants, supporting the hypothesis that the striatum functions as a general calorie sensor. However, the blunted striatal dopamine response to intragastric lipid, but not to glucose, in participants with obesity, points to impaired lipid sensing in nutrient-specific pathways that are involved in dopamine release.

Post-ingestive brain responses are not related to circulating hormones

We observed substantial interindividual variation in the BOLD signal responses to intragastric glucose and lipid infusion (Fig. 4). Moreover, because it is largely unknown how nutrient-derived signals are relayed to the brain, we assessed whether the variation in brain activity can be explained by variation in postprandial levels of circulating nutrients or hormones. We found that changes in the striatal BOLD signal could not be predicted by changes in plasma glucose, insulin or ghrelin following the glucose or lipid infusion (Supplementary Table 4). In the lean participants, plasma GLP-1 excursions correlated negatively with changes in BOLD signal after the lipid infusion in the putamen and caudate nucleus (Fig. 6a,b), indicating that GLP-1 release following intestinal exposure to lipids is associated with a decrease in striatal BOLD signal in lean individuals. We did not observe these correlations in the participants with obesity (Supplementary Table 4).

Discussion

In this study, we demonstrate the differential post-ingestive (that is, orosensory and preference-independent) effects of isocaloric intragastric glucose and lipids on neuronal activity in brain regions involved in the regulation of eating behaviour, as well as on striatal dopamine release in lean adults. Moreover, we show that most of these physiological responses to intragastric nutrients are impaired in humans with obesity, with no signs of reversibility after 12 weeks of dietary weight loss. Taken together, these findings support the hypotheses that: (i) glucose and lipid differentially affect brain regions involved in the regulation of eating behaviour through post-ingestive signals; (ii) impaired post-ingestive nutrient signalling may contribute to pathological eating behaviour, overeating and obesity; and (iii) the persistence of these disturbances after diet-induced weight loss may contribute to the high incidence of weight regain after dietary interventions.

Physiological brain responses to intragastric nutrients

Our unique study design, including the blinded administration of nutrients via nasogastric tube and the combination of state-of-the-art functional and molecular neuroimaging techniques, allowed us to evaluate the isolated post-ingestive effects of glucose and lipids on whole-brain neuronal activity and striatal dopamine release. By studying both lean participants and patients with obesity, we were able to first identify the physiological brain responses to intragastric glucose and lipids and subsequently determine that these responses are impaired in humans with obesity. Intragastric glucose and lipids swiftly and strongly alter brain activity in regions that have previously been implicated in the physiological regulation of eating behaviour[31–33]. Intriguingly, the spatial and temporal distribution of the responses differed substantially between the glucose and lipid infusions. Glucose administration had the most pronounced effects in the striatum and the frontal pole, regions involved in important aspects of eating behaviour, including reward expectancy and calculation, executive control and decision-making[31]. The effects of the lipid infusion were most notable in the insula and frontal cortex, regions involved in the integration of internal and external stimuli, the encoding of reinforcing stimuli and the regulation of reward-related behaviour[32,33]. In addition, we observed important changes in brain activity within the first 10 min following intragastric glucose, whereas most of the brain responses to intragastric lipids occurred after 20 min or more. As a study in lean humans showed that early gastric emptying (<45 min) did not differ between intragastric glucose and lipid[34], this temporal difference is unlikely to be explained by nutrient-specific differences in gastric emptying. We thus demonstrate that glucose and lipids have orosensory and preference-independent, yet nutrient-specific physiological effects on the central nervous system, suggesting that the signalling pathways by which the brain is informed about ingested nutrients may also be nutrient specific[3,7,13,35].

In addition to these nutrient-specific BOLD responses, we observed a similar striatal response to intragastric glucose and lipids. We were specifically interested in this region as it has been proposed to function as a post-ingestive caloric sensor and to play an important role in the adaptation of feeding behaviour to changes in the caloric

https://doi.org/10.1038/s42255-023-00816-9

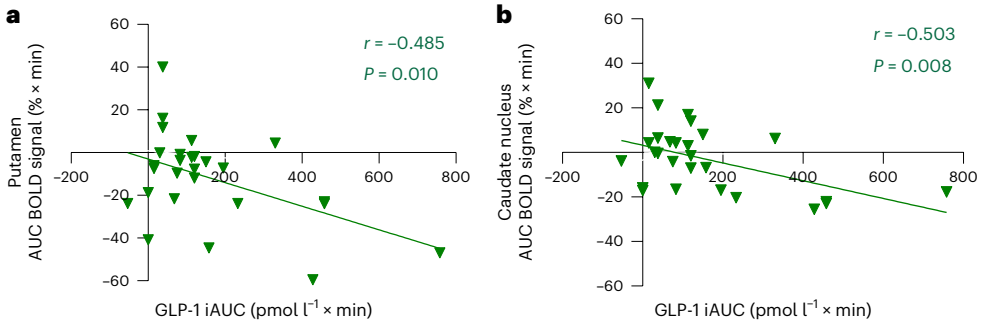

Fig. 6 | Strong GLP-1 release following intragastric lipids is associated with more pronounced changes in the striatal BOLD signal, only in lean participants. a,**b**, Scatterplots of the GLP-1 response to intragastric lipids versus changes in the BOLD signal in the putamen (**a**) and the caudate nucleus (**b**). Data are individual participants and were evaluated using Pearson's coefficient ($n = 27$). After Bonferroni correction, a two-tailed P value of 0.0125 was considered significant. The solid green line represents the regression line for the lean participants. Green symbols indicate lean participants. AUC, area under the curve; iAUC, incremental area under the curve.

value of energy intake[17]. In the lean individuals, intragastric glucose and lipids both decreased BOLD signals in the NAc and putamen and both resulted in striatal dopamine release. We thus extend the findings of rodent studies, showing striatal dopamine release following intragastric glucose or lipids[7,15], to healthy adults with normal body weight. Interestingly, in these rodent studies, the amount of striatal dopamine release correlated positively with the caloric load of the infusion, and the authors subsequently hypothesized the striatum to function as a general calorie sensor[17]. Although it goes beyond the scope of the present study to determine whether striatal dopamine release is directly related to caloric intake in humans, the similarity in the striatal response to isocaloric glucose or lipid infusions, but not to isovolumetric noncaloric water, points to a calorie-driven, rather than a nutrient-specific or volume-driven mechanism in this brain region.

We found that most of the post-ingestive cerebral changes were not associated with post-ingestive changes in circulating glucose or hormones, suggesting that cerebral post-ingestive nutrient signalling is not directly modified by these metabolic signals. However, linear correlation analyses might be less suited to studying the complex dynamics between post-ingestive nutritional signals and activity of specific neuronal circuits. In addition, postprandial nutrient availability might be sensed in the portal vein instead of in the systemic circulation[13]. Nevertheless, some of the interindividual variation in the lipid-induced striatal BOLD response could be explained by variation in GLP-1 release upon lipid infusion. The exact mechanisms underlying the anorexigenic effects of GLP-1 remain to be elucidated[36]: possible ways by which this gut hormone may indirectly affect the striatum include paracrine stimulation of intestinal vagal nerve afferents that then project to the brainstem and onwards to the striatum[37], endocrine stimulation of GLP-1 receptors in brain regions that are connected with the striatum[38,39] or direct action on striatal GLP-1 receptors[40].

Central nutrient resistance in people with obesity

In contrast to the physiological effects we observed in the lean participants, in the participants with obesity the whole-brain voxel-wise analysis and the NAc ROI analysis showed no functional responses to intragastric glucose or lipids. These findings are important, because the NAc is involved in the incentive, reinforcing and motivational aspects of (anticipatory) food cues and closely interacts with the homeostatic regulatory circuitry[41–44]. In humans, increases in NAc activity provoked by visual food stimuli predict greater subsequent ad libitum food intake[45], while a decrease in NAc activity correlates with reduced food palatability ratings[46]. In the present study, we therefore speculate that the observed nutrient-induced decrease in NAc BOLD signal in lean participants reflects a homeostatic response intended to devalue, and thus discourage, further food intake, because homeostatic needs have already been met. We further suggest that an absence of such a response, as observed in the participants with obesity, may lead to an inability to devalue the rewarding aspects of additional food intake, thereby promoting the consumption of food beyond homeostatic needs.

Whereas the absence of whole-brain and NAc functional responses to intragastric glucose and lipid in participants with obesity suggests a general defect in the sensing of post-ingestive nutrient signals, the observation that the functional response of the putamen and the striatal dopamine response were only impaired for intragastric lipids, but not glucose, indicates a specific defect in post-ingestive lipid sensing/signalling in these hedonic brain areas. In this regard, post-ingestive glucose versus lipids likely signals to the striatum via different pathways[3]. In rodents, the lipid-induced striatal response depended on a functioning vagal nerve[7]. When fed a high-fat diet, mice exhibited impaired striatal dopamine release in response to intragastric lipids[18], similarly to our participants with obesity. This was attributed to reduced intestinal synthesis of oleoylethanolamine[18], a bioactive lipid metabolite that interacts with vagal sensory afferents[47,48], and it will be highly relevant to determine if reduced intestinal oleoylethanolamine synthesis plays a role in human obesity development. Furthermore, a high-fat diet affected Agouti-related peptide (AgRP) neurons in mice[49]. This neuronal population in the hypothalamus has a critical role in the regulation of energy homeostasis and the transmission of homeostatic energy signalling to striatal dopamine signalling[50,51]. A negative energy status activates AgRP neurons to increase caloric intake[52,53], whereas intragastric nutrients inhibit these neurons and stimulate striatal dopamine release[51,54]. However, in mice following a high-fat diet, the inhibition of AgRP neurons by intragastric fat specifically was blunted and it would be interesting to study if this mechanism translates to human obesity[49]. The glucose-induced response, on the other hand, primarily relied on a vagal-independent mechanism (that is, portal-mesenteric sensing of glucose)[13]. Finally, a response within the putamen has been linked to the caloric value of nutrients and likely contributes to homeostatic feedback after food intake[17,55]. Thus, in the participants with obesity, an impaired putamen response to intragastric lipids may facilitate continued energy consumption after a lipid-rich meal.

To summarize, human obesity is associated with both global and nutrient-specific defects in post-ingestive nutrient sensing. These impairments may contribute to overeating (and subsequent weight gain) and provide future targets for the development of therapies against obesity.

Effects of diet-induced weight loss on brain responses

As we have previously shown that bariatric weight loss partially reversed obesity-associated alterations in the striatal dopamine system[22],

we hypothesized that dietary weight loss also reverses such impairments. Here, however, we show that a 12-week supervised dietary intervention promotes significant weight loss and metabolic improvement, but does not restore the physiological brain response to post-ingestive glucose or lipids in humans with obesity, at least during the time course of this study. We reported earlier on a significant increase in striatal $D_{2/3}R$ availability upon weight loss[22], but in that study weight loss was higher and induced by bariatric surgery and the interval between baseline and follow-up SPECT was 2 years compared to 12 weeks in the current study. Whether these systems are restored with long-term weight loss remains to be determined. Unfortunately, in practice, it may never come to this, because most patients regain weight within a few years of dieting: one meta-analysis of long-term weight loss trials showed that 50% of original weight loss was regained after 2 years and 80% after 5 years[56]. On the basis of the present study, we now postulate that persistent defects in post-ingestive nutrient signalling to the brain contribute to weight regain after dietary weight loss. If shown to be true, this would make these impairments even more appealing therapeutic targets, not only for weight loss but also for weight maintenance.

Limitations

Some nuances with respect to our findings should be made. Firstly, due to radiation exposure, we only studied individuals over 40 years of age, and we cannot extrapolate our findings to younger adults. Secondly, we performed continued fMRI scanning up to 32 min after the start of the intragastric infusions, so our conclusions are limited to this timeframe. It is possible that any of the observed obesity-associated defects are not entirely absent but merely delayed. However, if the cerebral response to food intake is indeed delayed for more than 30 min, these results are still highly relevant, because defects within this timeframe may result in delayed meal termination and thus more energy consumption. Thirdly, a recent paper reported on the stimulatory effect of systemic rehydration on dopaminergic neuron activity in the ventral tegmental area (dopaminergic neurons in this brain area project to the ventral striatum) in water-deprived mice[57]. This suggests that the control isovolumetric and noncaloric intragastric water infusion in the participants of the current study might have triggered neuronal activity affecting the BOLD signal and/or dopamine release. This would imply that the water condition cannot serve as an optimal neutral control condition. Since all participants were allowed to drink water and were not dehydrated when the functional imaging was performed, we expect the effect of water on the imaging outcomes to be small. Of note, the described effects of water on neuronal activation in the mice were smaller when the mice were not water-deprived and the volume of intragastric water used in that study was higher (approximately 30% of daily requirements versus 12.5% in our study). Fourthly, we standardized the volume and caloric load of the intragastric glucose and lipid infusion for all participants. The infused 500 kcal represented 33.3% versus 29.3% of caloric need in the resting state (measured using indirect calorimetry) for lean participants and participants with obesity, respectively. Although this difference of 4% is small, we cannot exclude that this may have contributed to the outcome. Fifthly, we cannot rule out an effect of the passage of time between the pre-diet and post-diet intervention scans in the participants with obesity. It was not feasible to re-scan the lean participants. Finally, our conclusions on reversibility remain limited to this specific dietary weight loss intervention. It is possible that (some of) the defects in post-ingestive nutrient signalling may be (partially) reversible by altering the macronutrient content, meal timing or duration of the intervention.

Conclusion

Data from the current study demonstrate that glucose and lipids have distinct post-ingestive effects on brain activity in regions involved in the regulation of eating behaviour as well as on striatal dopamine release in lean, healthy adults. Moreover, we found that humans with obesity have severely impaired functional and neurochemical responses to post-ingestive nutrients, with no signs of reversibility after 12 weeks of (successful) dietary weight loss. Taken together, these observations provide insights into the physiology of human eating behaviour, and the pathophysiology of obesity. The lack of reversibility after significant weight loss suggests that the high rate of weight regain after successful weight loss is in part explained by ongoing resistance to post-ingestive nutrient signals.

Methods

Participants

Thirty participants with a healthy body weight and 30 participants with obesity were recruited from the general population in the Amsterdam metropolitan area (Fig. 2). Participants were eligible to participate if they: (i) were men aged 40–70 years or post-menopausal women aged 50–70 years, (ii) had either BMI ≤ 25 kg/m^2 (participants with a healthy body weight) or BMI ≥ 30 kg/m^2 (participants with obesity) and (iii) had stable weight (<10% weight change) for at least 3 months before the study assessments. Exclusion criteria were: (i) use of any medication, except for thyroid hormone, antihypertensive and/or lipid-lowering drugs; (ii) any somatic disorder, except for dyslipidaemia, hypertension and/or treated hypothyroidism; (iii) history of any psychiatric or eating disorder; (iv) lactose, gluten, soybean oil, egg or peanut intolerance; (v) shift work; (vi) irregular sleep habits; (vii) regular vigorous exercise (>3 h/week); (vii) restrained eaters; (viii) childhood onset of obesity (at age <4 years); (ix) substance abuse (smoking, alcohol >3 units/day, recreational drugs); (x) occupational radiation exposure; or (xi) any contraindication for MRI. All participants completed a medical evaluation, including history, physical examination and blood tests.

Study design

In this single-blinded, randomized, controlled, crossover study (Fig. 1a), lean participants underwent three fMRI sessions on three separate study days to assess the effects of glucose, lipids and tap water on cerebral neuronal activity. Participants with obesity underwent three fMRI study days before the start of a 12-week hypocaloric diet intervention and three fMRI study days after completion of this diet intervention to assess the effect of diet-induced body weight loss. A stratified randomization scheme was used to determine the order of the infusions for the fMRI study days. During the three fMRI study days after the diet, the same nutrient infusion order was used as the one before the diet.

In addition, all participants underwent two [^{123}I]IBZM SPECT study days to assess the post-ingestive nutrient effects of glucose and lipids on the striatal dopamine system. In lean participants, in random order, the effect of glucose was assessed during one SPECT study day and the effect of lipids was assessed during the other SPECT day. Due to radiation exposure, the number of SPECT study days a participant is allowed to undergo is limited to two. Therefore, in participants with obesity, the effect of either glucose (n = 15) or lipids (n = 15) on the striatal dopamine system was assessed both before and after the diet. All randomization and allocation procedures were performed using the GraphPad QuickCalcs website. Primary study outcomes were the effects of the intragastric nutrient infusions on cerebral neuronal activity and striatal dopamine release. Secondary study outcomes were the effects of the intragastric nutrient infusions on: glucoregulatory and gut hormone release and objective and participantive hunger scores. The protocol was approved by the Academic Medical Center medical ethics committee. All participants provided written informed consent in accordance with the Declaration of Helsinki. The study was prospectively registered in the Netherlands Trial Registry (http://www.trialregister.nl/: NTR7042). The trial was registered on 22 February 2018. One pilot fMRI was performed in one participant who was enrolled on 13 December 2017. The data of this one participant were only used to optimize the fMRI protocol and are not included in the paper. The data

of participants included in this clinical trial and paper were collected from March 2018 onwards.

Experimental procedures

Anthropometric measurements. Body weight and fat percentage were measured using a BOD POD (COSMED USA). REE was measured by indirect calorimetry (Vmax Encore 29, Carefusion). Daily energy expenditure was estimated as 1.3 × REE.

Diet intervention. After the baseline study days, participants with obesity enrolled in a supervised personalized dietary weight loss programme aimed at reducing body weight by 10% over 12 weeks. Individual daily caloric budget was calculated on the basis of REE, estimated daily activity and the required caloric deficit to lose 10% body weight in 12 weeks. The diet adhered to a minimum intake of 1 g protein per kg body weight and consisted of approximately 45% carbohydrates, 20% lipids and 35% proteins. Participants received weekly supervision by telephone and visited the clinic for consultation and measurement of body weight and REE after the first and second month of the diet. If weight loss deviated from an average of 0.8% per week, the diet was adjusted accordingly. Participants with <5% body weight loss at the end of the diet intervention were excluded from participation in the post-diet study procedures.

Intragastric infusions. To bypass the orosensory and preference-dependent effects of nutrient ingestion, participants received intragastric infusions via a nasogastric tube (Levin, 12FR). Participants were first familiarized with the tube placement during a training session. Then, during the fMRI and SPECT study days, the intragastric infusions consisted of 250 ml glucose 50% (125 g of glucose, 500 kcal), 250 ml Intralipid 20% (50 g of soybean oil, 500 kcal) or 250 ml tap water (non-caloric and isovolumetric control). The participants were blinded to the order of the infusions.

fMRI. ***Protocol.*** The effects of the intragastric infusions of glucose, lipids and tap water on cerebral neuronal activity were assessed using fMRI on three separate study days (Fig. 1b). A pilot fMRI was performed in one participant who underwent nasogastric tube placement with infusion of lipids to assess feasibility and optimize the protocol. The data of this participant were not included in the analysis. Participants were instructed to consume the same dinner (40% of daily energy expenditure) the evening before each fMRI study day. After an overnight fast, participants came to the imaging facility of the Amsterdam UMC, location AMC in the morning between 6:00 and 10:00 am (time of arrival was consistent for each participant). Thirty minutes before the intragastric infusion, the nasogastric tube was inserted. A cannula was inserted in the antecubital vein to enable repeated blood sampling during fMRI acquisition. An anatomical brain scan was acquired on the first fMRI study day. During the functional brain scans, baseline activity was measured for 8 min, after which the intragastric infusion of glucose, lipids or tap water was administered in 5 min. Imaging continued for another 27 min. Participants were instructed to lie as still as possible, to stay awake, and to keep their eyes open. Blood was drawn at select time points during the functional brain scans. Participants were asked to rate their feeling of hunger on a VAS ranging from 0 to 10 before the start of the fMRI and shortly after the fMRI was finished. Twenty minutes after the removal of the nasogastric tube and intravenous cannula, participants received a meal, consisting of a bowl of yoghurt (isocaloric vanilla or natural) mixed with muesli, and were asked to eat until satiated. The food was weighed before and after consuming the meal and the caloric intake was calculated as caloric content after versus before the meal.

Acquisition. Data were acquired using a 3.0T Philips MR Scanner (Philips Medical Systems) using a 32-channel receive-only head coil. An anatomical T1-weighted scan was obtained with the following scan parameters: TR/TE = 7.0/3.2 ms; FOV = 256 × 240 × 180 mm; voxel size = 1 × 1 × 1 mm. fMRI was acquired using a gradient echo planar imaging (EPI) sequence with the following scan parameters: TR/TE = 1,700/35 ms; FOV = 216 × 216 × 124 mm; voxel size = 2.7 × 2.7 × 2.7 mm; 1410 dynamics; MB factor = 2; SENSE = 1.7; scan duration = 40 min.

Data processing and analysis. fMRI data were preprocessed using FMRIPREP v1.2.3 (RRID: SCR_016216)[58,59]. Anatomical T1-weighted scans were normalized to MNI space. Preprocessing of the functional scans included motion correction (FLIRT), distortion correction (3dQwarp) and co-registration to the anatomical T1-weighted scans. The functional scans were then nonaggressively denoised using independent component analysis based Automatic Removal Of Motion Artifacts (AROMA) and spatially smoothed (6 mm FWHM). For details, see the Supplementary Information ('fMRI preprocessing').

Participant-level analysis was performed using the Functional Magnetic Resonance Imaging of the Brain (FMRIB) Software Library (FSL 6.0; http://www.fmrib.ox.ac.uk/fsl). The first three volumes from each functional scan were removed. The remaining 1,407 volumes were divided over 14 consecutive time bins: T0 (baseline, that is, the 5 min before the start of the intragastric infusion) and T1–T13 (each including consecutive 2–2.5-min intervals, with T1 beginning directly at the start of the intragastric infusion). First-level analysis was applied with the use of FMRI Expert Analysis Tool (FEAT) to compare T1–T13 with baseline (T0) within every functional brain scan[60]. The time course of the BOLD signal of the cerebrospinal fluid of each scan was extracted and included as a covariate to adjust for general, non-infusion-related changes in BOLD signal. Next, for each participant, the maps of T1–T13 of the water infusion session were subtracted from the maps of T1–T13 of the glucose and lipid infusion session. For each participant, this resulted in 13 maps for the glucose infusion and the lipid infusion that reflected the percentage change in BOLD signal from baseline (T0) for each time bin (T1–T13) for glucose and lipids, corrected for the effects of the infusion of tap water. These values were used as input for the group-level analyses: the explorative whole-brain voxel-wise analysis and the ROI analysis.

For the whole-brain voxel-wise analysis, clusters of grey-matter voxels that showed a significant increase or decrease from baseline (T0) for each time bin (T1–T13) were identified using Threshold Free Cluster Enhancement and permutation testing using Permutation Analysis of Linear Models v.alpha116 (ref. 61). Faster permutation inference was applied by fitting a generalized Pareto distribution to the tail of the permutation distribution (*P* value threshold 0.10)[62], with 5,000 permutations. The Permutation Analysis of Linear Models options --corrcon and --corrmod were applied to perform FWER correction for multiple testing over the multiple contrasts and time bins, respectively[63]. A FWER-corrected *P* value (p_{FWER}) < 0.05 was considered significant. For clusters with a significant change in BOLD signal, the locations of the peak and up to five local maxima (minimum distance 20 mm) were interpreted using the Harvard–Oxford (sub)cortical atlas (https://fsl.fmrib.ox.ac.uk/fsl/fslwiki/Atlases/)[64–67]. As within-participant designs are more powerful than between-participant designs[68], this analysis was performed to assess the within-group effects of intragastric glucose and lipids in the lean participants and in the participants with obesity, in the pre-diet condition, separately. To evaluate the effect of the diet intervention, the voxel-wise analysis was performed on the post-diet data after subtraction of the pre-diet data for each participant.

For the ROI analysis, effects of the nutrient infusions on the striatal subregions the NAc, caudate nucleus and putamen were assessed with a ROI analysis. Masks of these regions were obtained from the Harvard–Oxford subcortical atlas (https://fsl.fmrib.ox.ac.uk/fsl/fslwiki/Atlases/)[64–67] with a threshold of 30%. The mean change (percentage) in BOLD signal from baseline (T0) was extracted for each time bin (T1–T13) for each ROI. To limit the number of comparisons, only at T3

(pre-absorption), T8 (early absorption) and T12 (late absorption), the significance of the change from baseline was evaluated by one-sample *t*-tests in lean participants and participants with obesity pre-diet. In addition, the effect of the diet intervention was evaluated by comparing the change from baseline for these time bins (T3, T8 and T12) between the pre-diet and post-diet conditions by paired *t*-tests.

SPECT. ***Protocol.*** The effects of the intragastric infusions of glucose and lipids on the striatal dopamine system were assessed using SPECT imaging with the radiotracer [^{123}I]IBZM (produced in accordance with GMP guidelines; GE Healthcare). [^{123}I]IBZM binds to the $D_{2/3}$R and competes with intrasynaptic dopamine for binding to $D_{2/3}$R. An acute decrease in the binding of [^{123}I]IBZM in the striatum indicates dopamine release[30]. After an overnight fast, participants came to the nuclear imaging facility of the Amsterdam UMC, location AMC between 8:00 and 9:00 am. The nasogastric tube was placed in accordance with the procedure of the training session. Via a cannula in the antecubital vein, an [^{123}I]IBZM bolus of 64 MBq was administered and a continuous infusion of 16 MBq h^{-1} was started for the duration of the experiment (5 h). The first SPECT scan started 2 h after the start of the [^{123}I]IBZM infusion and 45 min after the intragastric infusion of tap water (noncaloric isovolumetric control). The second SPECT scan started 4 h after the start of the [^{123}I]IBZM infusion and 45 min after the intragastric infusion of either glucose or lipids (Fig. 1c). A decrease in striatal [^{123}I]IBZM binding between the first and second SPECT scan is an indication of nutrient-induced striatal dopamine release. To limit thyroid uptake of free radioactive iodide, all participants were pretreated with potassium iodide.

Acquisition. SPECT imaging was performed using the InSPira HD system, a brain-dedicated SPECT camera (Neurologica) with the following parameters: matrix = 128 × 128; energy window = 135–190 keV; slice thickness = 4 mm; acquisition time per slice = 4 min; axial slices were acquired upward from and parallel to the orbitomeatal line until the whole striatum was covered.

Data processing and analysis. SPECT images were reconstructed with an iterative expectation maximization algorithm and corrected for attenuation by manually aligning an adult head template[69]. Binding of the radiotracer (that is, $D_{2/3}$R availability) was quantified for the striatum by an ROI analysis. Freesurfer (version 5.3.0) was used to obtain striatal masks from individual T1-weighted MRI scans. The occipital cortex was used as the reference region to quantify non-specific radiotracer activity. Occipital cortex masks were obtained by warping the occipital cortex from the Harvard–Oxford cortical atlas to individual T1-weighted MRI using FSL. For the striatum, $D_{2/3}$R availability (that is, non-displaceable binding potential (BP_{ND}) of [^{123}I]IBZM) was calculated as the specific-to-non-specific binding ratio: striatal BP_{ND} = (mean striatal binding − mean occipital cortex binding)/mean occipital cortex binding. Nutrient-induced changes in striatal $D_{2/3}$R availability were defined as BP_{ND} after the nutrient infusion (second SPECT scan), relative to BP_{ND} after the tap water infusion (first SPECT scan).

Registration of adverse events. We registered (serious) adverse events during the study. There were no serious adverse events and three adverse events during the study. Two participants experienced nausea after nasogastric tube placement and nutrient infusion (one lean participant and one participant with obesity), and one participant with obesity had transient worsening of pre-existent tinnitus. All adverse events were resolved. The MRI scans of these participants were excluded from the analyses. In the Supplementary Information ('missing data'), we describe these missing data.

Plasma nutrient and hormone measurements

During the fMRI session, blood was sampled at baseline and at 5, 10, 15, 20 and 30 min after the start of the intragastric infusion. Samples were centrifuged at 4 °C and stored at −80 °C. At all time points, plasma glucose was determined with the glucose oxidase method using a Biosen C-line plus glucose analyser (EKF Diagnostics). At baseline, $t = 15$ and $t = 30$, plasma insulin concentrations were determined by immunoassay (Luminescence, Atellica IM, Siemens Medical Solutions Diagnostics) with an intra-assay variation of 3%, inter-assay variation of 7% and lower limit of quantitation 10 pmol l^{-1}. In total, 2 mg ml^{-1} 4-(2-aminoethyl) benzenesulfonyl fluoride hydrochloride (AEBSF; Pefabloc SC; Roche) was added to EDTA tubes to prevent breakdown of acylated ghrelin. At baseline and $t = 30$, concentrations of plasma acylated ghrelin were determined by immunoassay (SPI-Bio A05106, SPI-Bio) with an intra-assay and inter-assay variation of 6% and lower limit of quantification of 4 pg l^{-1}. At baseline, $t = 15$ and $t = 30$ concentrations of plasma total GLP-1 were determined by radioimmunoassay (Merck Millipore) with an intra-assay and inter-assay variation of 9% and lower limit of quantitation of 5 pmol l^{-1}. The timing of the measurements was according to the known effects of nutrients on glucose, insulin and gut hormones[19,70,71].

Statistical analyses

Within-group post-ingestive nutrient-induced changes from baseline were evaluated by paired or one-sample *t*-tests. Between-group differences were evaluated by *t*-test, Mann–Whitney *U* test or Chi-square test or by two-way mixed ANOVA. The effects of the diet intervention were evaluated by paired *t*-tests or Wilcoxon signed-rank tests or by two-way repeated-measures ANOVA. BOLD signal time bins and time points of the glucose/hormone measurements were evaluated by calculating AUC and iAUC values using the trapezoidal method. Correlations between BOLD signal AUC and glucose/hormone iAUC were evaluated using Pearson's correlation coefficient. Findings were considered significant if $P < 0.05$. Assumptions of the statistical tests were met, and normality and equal variances were tested. Handling of missing data is described in the Supplementary Information. No statistical methods were used to predetermine sample sizes but our sample sizes are similar to those reported to be sufficient for within-subject comparisons in previous publications[72]. Statistical analyses were performed using IBM SPSS Statistics v26 and R v3.6.1.

Reporting summary

Further information on research design is available in the Nature Portfolio Reporting Summary linked to this article.

Data availability

Free access to individual data is restricted due to ethical/legal concerns. However, upon request, the data may be made available for scientific collaborations after the execution of appropriate data sharing agreements, after review and approval of requests by the medical ethics committee, participants and investigators in line with existing local/national regulations and data sharing agreements. Requests can be sent to the corresponding author. A first response to requests will follow within 4 weeks. Source data are provided with this paper.

Code availability

Computer codes used for data analyses will be published in a repository on GitHub: https://github.com/MJMSerlie/SPIN-Study.

References

1. Saper, C. B., Chou, T. C. & Elmquist, J. K. The need to feed: homeostatic and hedonic control of eating. *Neuron* **36**, 199–211 (2002).
2. Rossi, M. A. & Stuber, G. D. Overlapping brain circuits for homeostatic and hedonic feeding. *Cell Metab.* **27**, 42–56 (2018).
3. de Araujo, I. E., Schatzker, M. & Small, D. M. Rethinking food reward. *Annu. Rev. Psychol.* **71**, 139–164 (2020).

4. de Araujo, I. E. et al. Food reward in the absence of taste receptor signaling. *Neuron* **57**, 930–941 (2008).
5. Sclafani, A. & Glendinning, J. I. Flavor preferences conditioned in C57BL/6 mice by intragastric carbohydrate self-infusion. *Physiol. Behav.* **79**, 783–788 (2003).
6. Sclafani, A. & Ackroff, K. Flavor preferences conditioned by intragastric glucose but not fructose or galactose in C57BL/6J mice. *Physiol. Behav.* **106**, 457–461 (2012).
7. Han, W. et al. A neural circuit for gut-induced reward. *Cell* **175**, 665–678 (2018).
8. Berthoud, H. R. The vagus nerve, food intake and obesity. *Regul. Pept.* **149**, 15–25 (2008).
9. Fu, Z., Gilbert, E. R. & Liu, D. Regulation of insulin synthesis and secretion and pancreatic beta-cell dysfunction in diabetes. *Curr. Diabetes Rev.* **9**, 25–53 (2013).
10. Kreymann, B. et al. Glucagon-like peptide-1 7–36: a physiological incretin in man. *Lancet* **2**, 1300–1304 (1987).
11. Rindi, G. et al. Characterisation of gastric ghrelin cells in man and other mammals: studies in adult and fetal tissues. *Histochem Cell Biol.* **117**, 511–519 (2002).
12. Berthoud, H. R. Vagal and hormonal gut–brain communication: from satiation to satisfaction. *Neurogastroenterol. Motil.* **20**, 64–72 (2008).
13. Zhang, L. et al. Sugar metabolism regulates flavor preferences and portal glucose sensing. *Front Integr. Neurosci.* **12**, 57 (2018).
14. Berland, C. et al. Dietary lipids as regulators of reward processes: multimodal integration matters. *Trends Endocrinol. Metab.* **32**, 693–705 (2021).
15. Ren, X. et al. Nutrient selection in the absence of taste receptor signaling. *J. Neurosci.* **30**, 8012–8023 (2010).
16. Thanarajah, S. E. et al. Food intake recruits orosensory and post-ingestive dopaminergic circuits to affect eating desire in humans. *Cell Metab.* **29**, 695–706 (2019).
17. Ferreira, J. G. et al. Regulation of fat intake in the absence of flavour signalling. *J. Physiol.* **590**, 953–972 (2012).
18. Tellez, L. A. et al. A gut lipid messenger links excess dietary fat to dopamine deficiency. *Science* **341**, 800–802 (2013).
19. Little, T. J. et al. Mapping glucose-mediated gut-to-brain signalling pathways in humans. *Neuroimage* **96**, 1–11 (2014).
20. Lassman, D. J. et al. Defining the role of cholecystokinin in the lipid-induced human brain activation matrix. *Gastroenterology* **138**, 1514–1524 (2010).
21. Jones, R. B. et al. Functional neuroimaging demonstrates that ghrelin inhibits the central nervous system response to ingested lipid. *Gut* **61**, 1543–1551 (2012).
22. van der Zwaal, E. M. et al. Striatal dopamine D2/3 receptor availability increases after long-term bariatric surgery-induced weight loss. *Eur. Neuropsychopharmacol.* **26**, 1190–1200 (2016).
23. ter Horst, K. W. et al. Insulin resistance in obesity can be reliably identified from fasting plasma insulin. *Int J. Obes.* **39**, 1703–1709 (2015).
24. Tschop, M. et al. Circulating ghrelin levels are decreased in human obesity. *Diabetes* **50**, 707–709 (2001).
25. Korek, E. et al. Fasting and postprandial levels of ghrelin, leptin and insulin in lean, obese and anorexic subjects. *Prz. Gastroenterol.* **8**, 383–389 (2013).
26. Nelson, K. M. et al. Prediction of resting energy expenditure from fat-free mass and fat mass. *Am. J. Clin. Nutr.* **56**, 848–856 (1992).
27. Matthews, D. R. et al. Homeostasis model assessment: insulin resistance and beta-cell function from fasting plasma glucose and insulin concentrations in man. *Diabetologia* **28**, 412–419 (1985).
28. Flint, A. et al. Reproducibility, power and validity of visual analogue scales in assessment of appetite sensations in single test meal studies. *Int. J. Obes. Relat. Metab. Disord.* **24**, 38–48 (2000).
29. Ogawa, S. et al. Intrinsic signal changes accompanying sensory stimulation: functional brain mapping with magnetic resonance imaging. *Proc. Natl Acad. Sci. USA* **89**, 5951–5955 (1992).
30. Booij, J. et al. Assessment of endogenous dopamine release by methylphenidate challenge using iodine-123 iodobenzamide single-photon emission tomography. *Eur. J. Nucl. Med.* **24**, 674–677 (1997).
31. Berthoud, H. R., Lenard, N. R. & Shin, A. C. Food reward, hyperphagia, and obesity. *Am. J. Physiol. Regul. Integr. Comp. Physiol.* **300**, R1266–R1277 (2011).
32. Rolls, E. T. The functions of the orbitofrontal cortex. *Brain Cogn.* **55**, 11–29 (2004).
33. Frank, S., Kullmann, S. & Veit, R. Food-related processes in the insular cortex. *Front. Hum. Neurosci.* **7**, 499 (2013).
34. Goetze, O. et al. The effect of macronutrients on gastric volume responses and gastric emptying in humans: a magnetic resonance imaging study. *Am. J. Physiol. Gastrointest. Liver Physiol.* **292**, G11–G17 (2007).
35. Goldstein, N. et al. Hypothalamic detection of macronutrients via multiple gut–brain pathways. *Cell Metab.* **33**, 676–687 (2021).
36. Krieger, J. P. Intestinal glucagon-like peptide-1 effects on food intake: physiological relevance and emerging mechanisms. *Peptides* **131**, 170342 (2020).
37. Abbott, C. R. et al. The inhibitory effects of peripheral administration of peptide YY(3-36) and glucagon-like peptide-1 on food intake are attenuated by ablation of the vagal–brainstem–hypothalamic pathway. *Brain Res.* **1044**, 127–131 (2005).
38. Kastin, A. J., Akerstrom, V. & Pan, W. Interactions of glucagon-like peptide-1 (GLP-1) with the blood–brain barrier. *J. Mol. Neurosci.* **18**, 7–14 (2002).
39. Orskov, C. et al. Glucagon-like peptide I receptors in the subfornical organ and the area postrema are accessible to circulating glucagon-like peptide I. *Diabetes* **45**, 832–835 (1996).
40. Dickson, S. L. et al. The glucagon-like peptide 1 (GLP-1) analogue, exendin-4, decreases the rewarding value of food: a new role for mesolimbic GLP-1 receptors. *J. Neurosci.* **32**, 4812–4820 (2012).
41. Taha, S. A. & Fields, H. L. Encoding of palatability and appetitive behaviors by distinct neuronal populations in the nucleus accumbens. *J. Neurosci.* **25**, 1193–1202 (2005).
42. Baldo, B. A. & Kelley, A. E. Discrete neurochemical coding of distinguishable motivational processes: insights from nucleus accumbens control of feeding. *Psychopharmacol.* **191**, 439–459 (2007).
43. Berridge, K. C. et al. The tempted brain eats: pleasure and desire circuits in obesity and eating disorders. *Brain Res.* **1350**, 43–64 (2010).
44. O'Connor, E. C. et al. Accumbal D1R neurons projecting to lateral hypothalamus authorize feeding. *Neuron* **88**, 553–564 (2015).
45. Lawrence, N. S. et al. Nucleus accumbens response to food cues predicts subsequent snack consumption in women and increased body mass index in those with reduced self-control. *Neuroimage* **63**, 415–422 (2012).
46. Tiedemann, L. J. et al. Central insulin modulates food valuation via mesolimbic pathways. *Nat. Commun.* **8**, 16052 (2017).
47. de Rodriguez, F. R. et al. An anorexic lipid mediator regulated by feeding. *Nature* **414**, 209–212 (2001).
48. Schwartz, G. J. et al. The lipid messenger OEA links dietary fat intake to satiety. *Cell Metab.* **8**, 281–288 (2008).
49. Beutler, L. R. et al. Obesity causes selective and long-lasting desensitization of AgRP neurons to dietary fat. *eLife* **9**, e55909 (2020).
50. Gropp, E. et al. Agouti-related peptide-expressing neurons are mandatory for feeding. *Nat. Neurosci.* **8**, 1289–1291 (2005).

51. Reichenbach, A. et al. Metabolic sensing in AgRP neurons integrates homeostatic state with dopamine signalling in the striatum. *eLife* **11**, e72668 (2022).
52. Hahn, T. M. et al. Coexpression of Agrp and NPY in fasting-activated hypothalamic neurons. *Nat. Neurosci.* **1**, 271–272 (1998).
53. Aponte, Y., Atasoy, D. & Sternson, S. M. AGRP neurons are sufficient to orchestrate feeding behavior rapidly and without training. *Nat. Neurosci.* **14**, 351–355 (2011).
54. Su, Z., Alhadeff, A. L. & Betley, J. N. Nutritive, post-ingestive signals are the primary regulators of AgRP neuron activity. *Cell Rep.* **21**, 2724–2736 (2017).
55. Small, D. M. et al. Changes in brain activity related to eating chocolate: from pleasure to aversion. *Brain* **124**, 1720–1733 (2001).
56. Hall, K. D. & Kahan, S. Maintenance of lost weight and long-term management of obesity. *Med. Clin. North Am.* **102**, 183–197 (2018).
57. Grove, J. C. R. et al. Dopamine subsystems that track internal states. *Nature* **608**, 374–380 (2022).
58. Esteban, O. et al. Analysis of task-based functional MRI data preprocessed with fMRIPrep. *Nat. Protoc.* **15**, 2186–2202 (2020).
59. Esteban, O. et al. fMRIPrep: a robust preprocessing pipeline for functional MRI. *Nat. Methods* **16**, 111–116 (2019).
60. Woolrich, M. W. et al. Temporal autocorrelation in univariate linear modeling of fMRI data. *Neuroimage* **14**, 1370–1386 (2001).
61. Winkler, A. M. et al. Permutation inference for the general linear model. *Neuroimage* **92**, 381–397 (2014).
62. Winkler, A. M. et al. Faster permutation inference in brain imaging. *Neuroimage* **141**, 502–516 (2016).
63. Winkler, A. M. et al. Non-parametric combination and related permutation tests for neuroimaging. *Hum. Brain Mapp.* **37**, 1486–1511 (2016).
64. Frazier, J. A. et al. Structural brain magnetic resonance imaging of limbic and thalamic volumes in pediatric bipolar disorder. *Am. J. Psychiatry* **162**, 1256–1265 (2005).
65. Goldstein, J. M. et al. Hypothalamic abnormalities in schizophrenia: sex effects and genetic vulnerability. *Biol. Psychiatry* **61**, 935–945 (2007).
66. Makris, N. et al. Decreased volume of left and total anterior insular lobule in schizophrenia. *Schizophr. Res.* **83**, 155–171 (2006).
67. Desikan, R. S. et al. An automated labeling system for subdividing the human cerebral cortex on MRI scans into gyral based regions of interest. *Neuroimage* **31**, 968–980 (2006).
68. Cremers, H. R., Wager, T. D. & Yarkoni, T. The relation between statistical power and inference in fMRI. *PLoS ONE* **12**, e0184923 (2017).
69. Adriaanse, S. M. et al. Clinical evaluation of [^{123}I]FP-CIT SPECT scans on the novel brain-dedicated InSPira HD SPECT system: a head-to-head comparison. *EJNMMI Res.* **8**, 85 (2018).
70. Wolnerhanssen, B. K. et al. Dissociable behavioral, physiological and neural effects of acute glucose and fructose ingestion: a pilot study. *PLoS ONE* **10**, e0130280 (2015).
71. Lean, M. E. & Malkova, D. Altered gut and adipose tissue hormones in overweight and obese individuals: cause or consequence? *Int. J. Obes.* **40**, 622–632 (2016).
72. Thirion, B. et al. Analysis of a large fMRI cohort: statistical and methodological issues for group analyses. *Neuroimage* **35**, 105–120 (2007).
73. Grabner, G. et al. Symmetric atlasing and model based segmentation: an application to the hippocampus in older adults. *Med. Image Comput. Comput. Assist. Interv.* **9**, 58–66 (2006).

Acknowledgements

We acknowledge the volunteers who participated in our study, and the magnetic resonance and SPECT technicians and students for their assistance during the study. We also thank J. Hillebrand from the Laboratory of Endocrinology for assistance with the GLP-1 and ghrelin assays. J.B. is supported by NWO ZonMw medium-sized investments grant 16366. G.J.S. is supported by the National Institutes of Health grant P30DK026687. M.J.S. received an unrestricted research grant from Mediq-TEFA bv.

Author contributions

Conceptualization, K.A.G., K.W.H., S.E.F., J.B. and M.J.S.; methodology, K.A.G., A.S., K.W.H., S.E.F., J.B. and M.J.S.; software, K.A.G. and A.S.; investigation and formal analysis, K.A.G. and A.S.; writing—original draft, K.A.G.; writing—review and editing, A.S., K.W.H., S.E.F., J.B., R.T.C., G.J.S., R.J.D. and M.J.S.; visualization, K.A.G., A.S. and K.W.H.; supervision, K.W.H. and M.J.S.; project administration, K.A.G.; funding acquisition, M.J.S.

Competing interests

The authors declare no competing interests.

Additional information

Supplementary information The online version contains supplementary material available at https://doi.org/10.1038/s42255-023-00816-9.

Correspondence and requests for materials should be addressed to Mireille J. Serlie.

Peer review information *Nature Metabolism* thanks Alexandra DiFeliceantonio, Kathleen Page and the other, anonymous, reviewer(s) for their contribution to the peer review of this work. Primary Handling Editor: Ashley Castellanos-Jankiewicz, in collaboration with the *Nature Metabolism* team.

Reprints and permissions information is available at www.nature.com/reprints.

Publisher's note Springer Nature remains neutral with regard to jurisdictional claims in published maps and institutional affiliations.

[1]Amsterdam UMC, location AMC, Department of Radiology and Nuclear Medicine, Amsterdam, the Netherlands. [2]Amsterdam University Medical Centers (UMC), location AMC, Department of Endocrinology and Metabolism and Amsterdam Gastroenterology Metabolism Endocrinology Institute, Amsterdam, the Netherlands. [3]Amsterdam UMC, location AMC, Department of Clinical Chemistry, Laboratory of Endocrinology, Amsterdam, the Netherlands. [4]Yale University School of Medicine, Department of Radiology and Biomedical Imaging, New Haven, CT, USA. [5]Albert Einstein College of Medicine, Fleischer Institute for Diabetes and Metabolism, Bronx, NY, USA. [6]Yale University School of Medicine, Department of Psychiatry, New Haven, CT, USA. [7]Yale University School of Medicine, Department of Endocrinology, New Haven, CT, USA. ✉e-mail: mireille.serlie@yale.edu

nature portfolio

Corresponding author(s): M.J. Serlie

Last updated by author(s): Apr 16, 2023

Reporting Summary

Nature Portfolio wishes to improve the reproducibility of the work that we publish. This form provides structure for consistency and transparency in reporting. For further information on Nature Portfolio policies, see our Editorial Policies and the Editorial Policy Checklist.

Statistics

For all statistical analyses, confirm that the following items are present in the figure legend, table legend, main text, or Methods section.

n/a	Confirmed	
☐	☒	The exact sample size (*n*) for each experimental group/condition, given as a discrete number and unit of measurement
☐	☒	A statement on whether measurements were taken from distinct samples or whether the same sample was measured repeatedly
☐	☒	The statistical test(s) used AND whether they are one- or two-sided *Only common tests should be described solely by name; describe more complex techniques in the Methods section.*
☐	☒	A description of all covariates tested
☐	☒	A description of any assumptions or corrections, such as tests of normality and adjustment for multiple comparisons
☐	☒	A full description of the statistical parameters including central tendency (e.g. means) or other basic estimates (e.g. regression coefficient) AND variation (e.g. standard deviation) or associated estimates of uncertainty (e.g. confidence intervals)
☐	☒	For null hypothesis testing, the test statistic (e.g. *F*, *t*, *r*) with confidence intervals, effect sizes, degrees of freedom and *P* value noted *Give P values as exact values whenever suitable.*
☒	☐	For Bayesian analysis, information on the choice of priors and Markov chain Monte Carlo settings
☒	☐	For hierarchical and complex designs, identification of the appropriate level for tests and full reporting of outcomes
☐	☒	Estimates of effect sizes (e.g. Cohen's *d*, Pearson's *r*), indicating how they were calculated

Our web collection on statistics for biologists contains articles on many of the points above.

Software and code

Policy information about availability of computer code

Data collection	The online randomization tool available on http://www.graphpad.com/quickcalcs/index.cfm was used for the randomization and allocation procedures.
Data analysis	fMRI data were preprocessed using FMRIPREP v1.2.3. Subject level analysis was performed using the Functional Magnetic Resonance Imaging of the Brain (FMRIB) Software Library (FSL 6.0, Oxford, UK). Whole-brain voxel-wise analysis was performed using Permutation Analysis of Linear Models (PALM) v.alpha116. Freesurfer (version 5.3.0) was used to obtain ROI masks from individual T1w MRI scans. Statistical analyses were performed using IBM SPSS Statistics v26 (Armonk, NY, USA) and R v3.6.1. Computer codes used for data analyses will be published in on the GitHub platform: https://github.com/MJMSerlie/SPIN-Study.

For manuscripts utilizing custom algorithms or software that are central to the research but not yet described in published literature, software must be made available to editors and reviewers. We strongly encourage code deposition in a community repository (e.g. GitHub). See the Nature Portfolio guidelines for submitting code & software for further information.

Data

Policy information about availability of data

All manuscripts must include a data availability statement. This statement should provide the following information, where applicable:

- Accession codes, unique identifiers, or web links for publicly available datasets
- A description of any restrictions on data availability
- For clinical datasets or third party data, please ensure that the statement adheres to our policy

Individual data (subject characteristics) were entered in a Castor database; laboratory results were entered into a hospital based electronic record (EPIC).
Masks of ROIs were obtained from the Harvard-Oxford subcortical atlas (https://fsl.fmrib.ox.ac.uk/fsl/fslwiki/Atlases). Subject level analysis was performed using the Functional Magnetic Resonance Imaging of the Brain (FMRIB) Software Library (FSL 6.0, Oxford, UK; http://www.fmrib.ox.ac.uk/fsl).
Free access to the individual data is restricted due to ethical/legal concerns. However, upon request the data may be made available for scientific collaborations after the execution of appropriate data sharing agreements, after review and approval of requests by the medical ethics committee, participants and investigators in line with existing local/national regulations and data sharing agreements. Requests can be send to the corresponding author (Mireille J. Serlie - mireille.serlie@yale.edu). A first response to requests will follow within 4 weeks.

Human research participants

Policy information about studies involving human research participants and Sex and Gender in Research.

Reporting on sex and gender	We included female and male subjects. The study has not enough statistical power to perform a valid analysis between sexes. To minimize sex differences with regard to the effect of sex hormones, we only included postmenopausal women. We did not collect any gender data.
Population characteristics	Shown in detail in Table 1.
Recruitment	Participants were recruited from the general population in the Amsterdam metropolitan area via local advertisements. There was no self-selection bias regarding inclusion of participants or study design. Subjects included in this trial might not be representative for the general population, subjects < 50 years (due to the restriction of exposing healthy and younger subjects to procedures involving radiation) and premenopausal women because of strict exclusion criteria.
Ethics oversight	The protocol was approved by the Academic Medical Center medical ethics committee.

Note that full information on the approval of the study protocol must also be provided in the manuscript.

Field-specific reporting

Please select the one below that is the best fit for your research. If you are not sure, read the appropriate sections before making your selection.

☒ Life sciences ☐ Behavioural & social sciences ☐ Ecological, evolutionary & environmental sciences

For a reference copy of the document with all sections, see nature.com/documents/nr-reporting-summary-flat.pdf

Life sciences study design

All studies must disclose on these points even when the disclosure is negative.

Sample size	There has been substantial debate in the field regarding the power and statistical analysis of fMRI data. Between-group analyses are complicated by the large inter-subject variability in brain activity assessed by fMRI. The between-subject variability is caused by a mixture of random and deterministic or structured factors that are not easily studied and hard to predict. This unpredictable inter-subject variability complicates sample size calculation for fMRI studies. Therefore, the necessary sample size to reliably evaluate intervention effects on brain activity between groups has been an active topic of research, and conventional sample size calculations are no longer recommended for studies where fMRI outcomes are a primary objective. One analysis suggested that functional neuroimaging studies should include at least 27 subjects per treatment group to have sufficient power for inter-group analyses. Another study performed subsample analyses (consisting of a variable number of subjects selected from the total population of 130 subjects) to determine the effect of sample size on the precision of task outcomes. This showed that by increasing the sample size from 20 to 30 (i.e. selected from the total population), the precision of the outcome estimation increased substantially: outcomes in n = 30 subsamples correlated 95% with outcomes in the total population, and this was associated with a variance of 0.0002 in the outcome between different compositions of the 30/120 subsample. On the basis of these insights, in order to reliably assess inter-group differences in the effects of nutrients on brain activity, we intended to include 30 subjects per group: 30 lean and 30 subjects with obesity. However, since then new reports showed that this number of subjects is sufficient to reliably assess within-subject differences, but not between-subject differences. We therefore assessed the within-group effects of intragastric glucose and lipids in the lean subjects and in the subjects with obesity separately.

The main aim of the SPECT scan procedures in lean subjects was to compare the nutrient (glucose and Intralipid) effects on striatal dopamine release. We expected both glucose and intralipid to induce striatal dopamine release. No previous study assessed the effect of nutrient infusion on striatal IBZM BPnd (measure of dopamine release). Consumption of a meal resulted in a 12.4% decrease of [11C]raclopride BPnd in the putamen. Using this effect size, a sample size of n=27 with a power of 80% (paired t-test) was needed. Since the radiotracer [11C]raclopride is slightly more sensitive to fluctuations in endogenous dopamine (due to a lower affinity for the dopamine receptor), we included a total of 30 lean subjects.

The main aim of the SPECT scan procedures in the subjects with obesity was to assess the effect of dietary weight loss on dopamine release induced by glucose or Intralipid. To our knowledge this has not been studied previously. Therefore we used study results from another study from our group with a similar population for this sample size calculation. Weight loss in that study induced a 15-16% increase in striatal BPnd. The standard deviation of the difference in BPnd before and after weight loss was 0.087 (arbitrary units). It follows that a sample size of n=15 has a power of 80% to find a difference in BPnd of 0.068 (arbitrary units). This translates to a difference of ±10% in basal BPnd. We considered this difference to be clinically relevant. We therefore included n=15 subjects with obesity per nutrient infusion group (i.e. 15 subjects for glucose infusion and 15 subjects for Intralipid infusion).

Data exclusions

Exclusion criteria were predefined, for details we refer to our method section.
Primarily due to the invasive nature of some of our study procedures, we have some missing data. Two lean subjects dropped out during the first fMRI session, before any of the SPECT study days. One lean subject and one subject with obesity completed only one fMRI session, but did complete all SPECT study days. In two subjects with obesity, the pre-diet, lipid fMRI session was interrupted and excluded from the analysis. One lean subject did not undergo the lipid SPECT session, whereas another lean subject did not undergo the glucose SPECT session. One subject with obesity did not continue with the diet intervention. Three subjects with obesity did not achieve >5% weight loss during the hypocaloric diet intervention and did not participate in post-diet study procedures. The post-diet, lipid fMRI session was interrupted in one subject and the glucose session in another. Finally, one subject's post-diet lipid SPECT session could not be completed due to technical failure of the scanner. For some subjects the sampling of blood during the fMRI session did not succeed due to failure of the iv cannula. We refer to the precise 'n' values in Figure 3.
Therefore, fMRI data could be analyzed for 27 lean subjects (both glucose and lipid) for 29 and 27 pre-diet subjects with obesity (glucose and lipid, resp.), and for 25 and 25 post-diet subjects (glucose and lipid, resp.). The SPECT data could be analyzed for 27 lean subjects (both glucose and lipid), for 30 pre-diet subjects with obesity (15 glucose and 15 lipid), and for 14 and 11 post-diet subjects (glucose and lipid, resp.). For an overview, we refer to Figure 2 (participant flow chart).

Replication

No replication was done. Due to the invasive nature of the study procedures (i.e. insertion of a nasogastric tube, radiation exposure) it was not considered ethical to increase the number of study procedures per participant any further.

Randomization

The order of the infusions for the fMRI study days was randomized and stratified by group. Subjects with obesity, were randomized to receive either intragastric glucose (n=15) or lipids (n=15) during SPECT study days. All randomization and allocation procedures were performed using the GraphPad QuickCalcs website.

Blinding

Participants were blinded for the type of intragastric infusion they received.

Reporting for specific materials, systems and methods

We require information from authors about some types of materials, experimental systems and methods used in many studies. Here, indicate whether each material, system or method listed is relevant to your study. If you are not sure if a list item applies to your research, read the appropriate section before selecting a response.

Materials & experimental systems

n/a	Involved in the study
☒	☐ Antibodies
☒	☐ Eukaryotic cell lines
☒	☐ Palaeontology and archaeology
☒	☐ Animals and other organisms
☐	☒ Clinical data
☒	☐ Dual use research of concern

Methods

n/a	Involved in the study
☒	☐ ChIP-seq
☒	☐ Flow cytometry
☐	☒ MRI-based neuroimaging

Clinical data

Policy information about clinical studies

All manuscripts should comply with the ICMJE guidelines for publication of clinical research and a completed CONSORT checklist must be included with all submissions.

Clinical trial registration

Trial registration: Netherlands Trial Registry NTR7042

Study protocol

Included with submission.

Data collection

A pilot fMRI was performed in one subject who underwent nasogastric tube placement with infusion of lipids to assess feasibility and optimize the fMRI protocol. This subject was enrolled on December 13 2017. The data of this subject is not included in the analysis. Thirty subjects with a healthy body weight and 30 subjects with obesity were recruited from the general population in the

Amsterdam metropolitan area. These subjects were enrolled from March 15 2018 to November 22 2019. Data of these subjects was collected from March 30 2018 to March 4 2020. All data was collected at the Amsterdam UMC, location AMC, in Amsterdam.

Outcomes

Primary study outcomes were the effects of the intragastric nutrient infusions on cerebral neuronal activity and striatal dopamine release. Secondary study outcomes were the effects of the intragastric nutrient infusions on: glucoregulatory and gut hormone release and objective and subjective hunger scores.
Lean subjects underwent three fMRI sessions on three separate study days to assess the effects of glucose, lipids, and tap water on cerebral neuronal activity. Subjects with obesity underwent three fMRI study days before the start of a 12-week hypocaloric diet intervention and three fMRI study days after completion of this diet intervention to assess the effect of diet-induced body weight loss.
In addition, all subjects underwent two [123I]IBZM SPECT study days to assess the post-ingestive nutrient effects of glucose and lipids on the striatal dopamine system. In lean subjects, in random order, the effect of glucose was assessed during one SPECT study day and the effect of lipids during the other SPECT day. Due to radiation exposure, the number of SPECT study days a subject is allowed to undergo is limited to two. Therefore, in subjects with obesity, the effect of either glucose (n=15) or lipids (n=15) on the striatal dopamine system was assessed both before and after the diet.
During the fMRI session, blood was sampled at baseline and at 5, 10, 15, 20, and 30 minutes after the start of the intra-gastric infusion. At all timepoints, plasma glucose was determined. At baseline, t=15, and t=30 plasma insulin and GLP-1 concentrations were determined. At baseline and t=30, concentrations of plasma acylated ghrelin were determined.
Subjects were asked to rate their feeling of hunger on a visual analogue scale (VAS) with a range from 0 to 10 before the start of the fMRI and shortly after the fMRI was finished. Twenty minutes after the removal of the nasogastric tube and i.v. cannula, subjects received a meal, consisting of a bowl of yoghurt (isocaloric vanilla or natural) mixed with muesli, and were asked to eat until satiated. The food was weighed before and after consuming the meal and the caloric intake was calculated as caloric content after versus before the meal.

Magnetic resonance imaging

Experimental design

Design type

Event-related (response to intra-gastric infusions).

Design specifications

During the functional brain scans, baseline activity was measured for eight minutes, after which the intragastric infusion of either glucose, lipids, or tap water was administered in five minutes. Imaging continued for another 27 minutes. Subjects had one fMRI session per day.

Behavioral performance measures

No behavioral performance measures were recorded during the functional brain scans.

Acquisition

Imaging type(s)

Functional.

Field strength

3T

Sequence & imaging parameters

TR/TE = 7.0/3.2ms; FOV = 256x240x180mm; voxel size = 1x1x1mm. fMRI was acquired using a gradient echo planar imaging (EPI) sequence with the following scan parameters: TR/TE = 1700/35ms; FOV = 216x216x124mm; voxel size = 2.7x2.7x2.7mm; 1410 dynamics; MB factor = 2; SENSE= 1.7; scan duration = 40 minutes.

Area of acquisition

Whole-brain.

Diffusion MRI ☐ Used ☒ Not used

Preprocessing

Preprocessing software

fMRI data were preprocessed using FMRIPREP v1.2.3 [RRID: SCR_016216]. Preprocessing of the functional scans included motion correction (FLIRT), distortion correction (3dQwarp), and co-registration to the anatomical T1-weighted scans. The functional scans were then non-aggressively denoised using independent component analysis (ICA) based Automatic Removal Of Motion Artifacts (AROMA) and spatially smoothed (6mm FWHM). For details see supplementary materials.

Normalization

Scans were spatially normalized to MNI space through nonlinear registration.

Normalization template

MNI space.

Noise and artifact removal

fMRI data were preprocessed using FMRIPREP v1.2.3[RRID: SCR_016216]. Anatomical T1-weighted scans were corrected for intensity non-uniformity, skull-stripped and spatially normalized to MNI space through nonlinear registration. In the brain-extracted T1-weighted image, brain tissue was segmented in CSF, white-matter (WM) and gray-matter (GM). Functional scans were corrected for motion (FLIRT) and distortion (TOPUP technique using 3dQwarp), and were co-registered to individual anatomical T1-weighted scans (boundary-based registration cost-function, 9 degrees of freedom). The motion correcting transformations, field distortion correcting warps, BOLD-to-T1-weighted transformations, and T1-weighted-to-MNI warp were performed with a single interpolation step using antsApplyTransforms (ANTs v2.1.0) with Lanczos interpolation. Independent component analysis (ICA) based on Automatic Removal Of Motion Artifacts (AROMA) was applied for non-aggressive denoising of the functional data. Finally, the functional data were spatially smoothened (6 mm full-width half-maximum).

Volume censoring

The first three volumes from each functional scan were removed.

Statistical modeling & inference

Model type and settings

Subject level analysis was performed using the Functional Magnetic Resonance Imaging of the Brain (FMRIB) Software Library (FSL 6.0, Oxford, UK; http://www.fmrib.ox.ac.uk/fsl). The first three volumes from each functional scan were removed. The remaining 1407 volumes were divided over 14 consecutive time bins: T0 (baseline, i.e. the 5 minutes before the start of the intragastric infusion) and T1-T13 (each including consecutive 2-2.5-minute intervals, with T1 beginning directly at the start of the intragastric infusion). First level analysis was applied with use of FMRI Expert Analysis Tool (FEAT) to compare T1-T13 with baseline (T0) within every functional brain scan. The time course of the BOLD signal of the cerebrospinal fluid (CSF) of each scan was extracted and included as covariate to adjust for general, non-infusion related changes in BOLD signal. Next, for each subject, the maps of T1-T13 of the water infusion session were subtracted from the maps of T1-T13 of the glucose and lipids infusion session. For each subject, this resulted in 13 maps for the glucose infusion and the lipid infusion that reflected the percentage change in BOLD signal from baseline (T0) for each time bin (T1-T13) for glucose and lipids, corrected for the effects of the infusion of tap water. These values were used as input for the group level analyses: the explorative whole-brain voxel-wise analysis and the ROI analysis.

Effect(s) tested

Whole-brain voxel-wise analysis - Clusters of grey-matter voxels that showed a significant increase or decrease from baseline (T0) for each time bin (T1-T13) were identified using Threshold Free Cluster Enhancement (TFCE) and permutation testing using Permutation Analysis of Linear Models (PALM) v.alpha116. Faster permutation inference was applied by fitting a generalized Pareto distribution to the tail of the permutation distribution, with 5000 permutations. The PALM options –corrcon and –corrmod were applied to perform FWER correction for multiple testing over the multiple contrasts and time bins, respectively. A FWER-corrected p-value (pFWER) <0.05 was considered significant. For clusters with a significant change in BOLD signal the locations of the peak and up to five local maxima (minimum distance 20mm) were interpreted using the Harvard-Oxford (sub)cortical atlas (https://fsl.fmrib.ox.ac.uk/fsl/fslwiki/Atlases). As within-subject designs are more powerful than between-subject design, this analysis was performed to assess the within-group effects of intragastric glucose and lipids in the lean subjects and in the subjects with obesity, pre-diet, separately. To evaluate the effect of the diet-intervention, the voxel-wise analysis was performed on the post-diet data after subtraction of the pre-diet data for each subject.

ROI analysis - Effects of the nutrient infusions on the striatal subregions the NAc, caudate nucleus, and putamen were assessed with a ROI analysis. Masks of these regions were obtained from the Harvard-Oxford subcortical atlas (https://fsl.fmrib.ox.ac.uk/fsl/fslwiki/Atlases) with a threshold of 30%. The mean change (%) in BOLD signal from baseline (T0) was extracted for each time bin (T1-T13) for each ROI. To limit the number of comparisons, only at T3 (pre-absorption), T8 (early-absorption) and T12 (late-absorption) the significance of the change from baseline was evaluated by one-sample t-tests in lean subjects and subjects with obesity pre-diet. In addition, the effect of the diet-intervention was evaluated by comparing the change from baseline for these time bins (T3, T8 and T12) between the pre and post-diet condition by paired t-tests.

Specify type of analysis: ☐ Whole brain ☐ ROI-based ☒ Both

Anatomical location(s)

For clusters with a significant change in BOLD signal the locations of the peak and up to five local maxima (minimum distance 20mm) were interpreted using the Harvard-Oxford (sub)cortical atlas (https://fsl.fmrib.ox.ac.uk/fsl/fslwiki/Atlases).

ROI masks were obtained from the Harvard-Oxford subcortical atlas (https://fsl.fmrib.ox.ac.uk/fsl/fslwiki/Atlases) with a threshold of 30%.

Statistic type for inference (See Eklund et al. 2016)

Clusters of grey-matter voxels that showed a significant increase or decrease from baseline (T0) for each time bin (T1-T13) were identified using Threshold Free Cluster Enhancement (TFCE) and permutation testing using Permutation Analysis of Linear Models (PALM) v.alpha116. Faster permutation inference was applied by fitting a generalized Pareto distribution to the tail of the permutation distribution, with 5000 permutations.

Correction

The PALM options –corrcon and –corrmod were applied to perform FWER correction for multiple testing over the multiple contrasts and time bins, respectively [61]. A FWER-corrected p-value (pFWER) <0.05 was considered significant.

Models & analysis

n/a	Involved in the study
☒	☐ Functional and/or effective connectivity
☒	☐ Graph analysis
☒	☐ Multivariate modeling or predictive analysis